An Advanced Numerical Model for Single Straight Tube Coriolis Flowmeters

Tao Wang, Roger C. Baker
(Department of Engineering, University of Cambridge, Cambridge, CB2 1RX, UK)
Yousif Hussain
(Krohne Ltd., Wellingborough, NN8 6AE, UK)

Abstract A detailed numerical model has been developed to simulate the single straight tube Coriolis flowmeter, which includes all important practical features. The measuring tube is modeled as fluid-tube interaction elements characterized as mass, stiffness and damping matrices based on the theories of fluid-structure interaction and finite element method. Other features, such as the inner and outer cases and the driver spring as in Krohne OPTIMASS flowmeters, are modeled as standard ANSYS beam and shell elements and coupled to the measuring tube. The modal frequency and phase shift from experiments are used to validate the model. In particular, our results show that the modal behaviour of the meter can only be adequately modeled if these practical features are included.

Keywords: Coriolis mass flowmeters, finite element, fluid structure interaction

1. Introduction

Single straight tube Coriolis flowmeters were first introduced to the market in the late 1980s and early 1990s. Since then, various hardware or software technologies have been applied to improve the effects of external mounting conditions and temperature variations. With these improvements, together with the intrinsic advantages of the meter (such as compactness, low pressure drop, self-draining, etc.), single straight tube meters have become an important option.

Raszillier and Durst [1] provided an analytical solution based on perturbation theory assuming a relatively small flow velocity compared with the critical velocity. In their recent work, Kutin and Bajisic [2] gave an analytical solution with a higher order of flow velocity by using the Galerkin method. Although these analytical solutions reflect the fundamental principle of Coriolis meters, they are limited to modal analysis of the measuring tube with simple geometry and boundary conditions.

Numerical methods, especially the finite element (FE) method, have been applied to investigate more complicated geometry and boundary conditions, or to conduct forced-response analyses [3-8]. Where analysis of single straight tube meters has been reported in the literature, they have been treated as simple straight fluid-conveying tubes with two clamped ends. However, modern designs of industrial flowmeters normally include other important features such as vibration compensation and stiffness modification mechanisms. This paper, therefore, considers a more complete and realistic numerical model of the industrial flowmeter design.

2. A practical design for single straight tube Coriolis flowmeters

One of the major design criteria for single straight tube flowmeters is the minimization of external mounting effects. Besides the measuring tube, the inner housing cylinder [9, 10] is an essential part of the flowmeter structure and has several requirements: it provides the rigid structure which clamps the ends of the fluid-conveying tube; it carries the driver and sensors to create and measure the vibration and Coriolis effect; it ensures that the tube is isolated from the neighbouring pipework through its compensation

capability.

In addition, a stiffness modification mechanism, such as a reinforcing spring [11], is important in improving the measurement performance. Such a spring acts on the measuring tube and modifies the frequency of the drive mode. Since the phase shift due to mass flow depends on the spectral distance between the drive mode and the nearby Coriolis mode, the sensitivity to mass flow rate can also be modified for a specific design purpose.

A schematic view of this design [9-11] is shown in Fig. 1. The measuring tube component is between points A_L and A_R. Although the principle of this practical design is similar to the situation assumed in previous work, where A_L and A_R were perfectly clamped, it is clear that the dynamic behaviour of the whole system will be different.

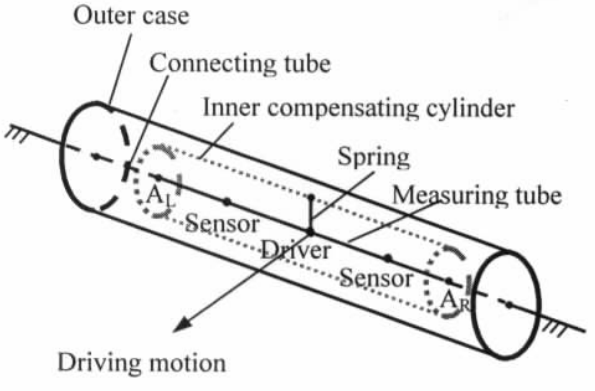

Fig. 1 A schematic view of a modern design

It is the objective of this paper to identify the difference in a quantitative way. The aim is to use this practical model as a simulation tool to improve the performance of the current product and to develop future products.

3. The finite element model

3.1. The formulation of the fluid-tube interaction element

In his book, Païdoussis [12] gave a detailed explanation and derivation of the governing equations of fluid-tube interaction. For single straight tube meters, as pointed out by Wang and Baker [8], the axial stress term is necessary. This term is included in the governing equations. In the plane of the driving motion, the equation of motion for the transverse deflection u and rotation θ at a specific point x and time t is given by

$$\begin{aligned}&(\rho_f A_f+\rho_p A_p)\frac{\partial^2 u}{\partial t^2}+2\rho_f A_f v_0\frac{\partial^2 u}{\partial x\partial t}\\&\quad+(\rho_f A_f v_0^2-\sigma_0 A_p)\frac{\partial^2 u}{\partial x^2}+kGA_p(\frac{\partial\theta}{\partial x}-\frac{\partial^2 u}{\partial x^2})=0\\&(\rho_f I_f+\rho_p I_p)\frac{\partial^2\theta}{\partial t^2}-kGA_p(\frac{\partial u}{\partial x}-\theta)-(E+\sigma_0)I_p\frac{\partial^2\theta}{\partial x^2}=0\end{aligned}\tag{1}$$

where the fluid in the tube is assumed to move with uniform and constant velocity v_0, in a tube of area A_f, to have density ρ_f, and to have a rotary inertia I_f; and where the conveying tube has an initial stress of σ_0, density ρ_p, cross-sectional area of A_p, rotary inertia I_p, Young's modulus E, shear modulus G, and shear correction factor k. Equation (1) is also valid for the other transverse motion perpendicular to the drive motion. It is worth noting that equation (1) is essentially a Timoshenko beam formulation, because the measuring tube is not necessarily slender enough for the validity of an Euler-Bernoulli beam formulation [12]. In addition, the axial and torsional motions follow the normal structural analysis. Therefore, in a 3D space each point has 6 degrees of freedom (DOF).

For the measuring tube alone, it is possible to solve equation (1) analytically. However, as shown in Fig. 1, there are other features coupled with the measuring tube. A finite element in its matrix form was developed to model the measuring tube so that it could be conveniently coupled with available finite elements. This fluid-tube interaction element uses a linear interpolation of displacement for axial and torsional DOFs separately, and a combined cubic interpolation for lateral and bending DOFs. This results in the matrix form of the partial differential equations. For a free vibration analysis,

$$\mathbf{M}^{(e)}\ddot{\mathbf{d}}+\mathbf{C}^{(e)}\dot{\mathbf{d}}+\mathbf{K}^{(e)}\mathbf{d}=0\tag{2}$$

where $\mathbf{d}$ is the vector of the nodal displacement, and $\mathbf{M}^{(e)}$, $\mathbf{C}^{(e)}$ and $\mathbf{K}^{(e)}$ represent one particular element e (e=1…n), which consists of two nodes and has a total of 12 degrees of freedom in a 3D coordinate system. For a forced-response analysis,

$$\mathbf{M}^{(e)}\ddot{\mathbf{d}}+\mathbf{C}^{(e)}\dot{\mathbf{d}}+\mathbf{K}^{(e)}\mathbf{d}=\mathbf{f}^{(e)}\tag{3}$$

where $\mathbf{f}^{(e)}$ is the driving force, for example on the driver position.

3.2. The implementation of the model

For all fluid-conveying tubes (the measuring tube, connecting tubes, and process pipes) of the flowmeter, the above matrices were used to model their dynamics. Along these tubes, the added rings were simply modeled as different sections. Matrix elements are provided by some commercial FE packages, which make the implementation convenient. We used the ANSYS Matrix27 element and its parametric language to calculate these matrices according to the flow and design parameters.

For the driver spring, a normal beam element was used. However, since the hollow measuring tube was modeled, essentially, as a 1D beam element, the connection between the measuring tube and the driver spring had to be coupled approximately. This coupling was investigated by comparing a full 3D dynamic FE analysis and the beam model. It was found that a rigid coupling region between the end of the driver spring and the centre of the tube gave a satisfactory result. With this coupling method, the agreement between 3D and beam models in terms of the resonant frequencies for the first 3 modes was better than 0.2%.

While it might be more accurate to model the inner compensating cylinder and outer case as 3D solid elements, this would involve too much computation time. Shell elements are found to be sufficient since we are not interested in their higher modes. The coupling method used for the measuring tube and inner cylinder, and for the connecting tube and outer case was a rigid region similar to the coupling between driver spring and measuring tube.

A section view of a complete model is shown in Fig. 2. To solve equation (2), ANSYS complex eigensolver [13] is used. With the calculated amplitude and phase for each node, the phase shift can be extracted as the difference between two sensor positions. It is worth noting that for each sensor the amplitude or phase is actually the relative movement between the corresponding points on the measuring tube and the inner cylinder. Because the meter is working under forced vibration, equation (3) is useful, especially for modeling zero shift due to small non-symmetrical configurations. To solve equation (3), a harmonic response analysis [13] was used.

3.3 Material damping

In the damping matrix of equations (2) or (3), only the effects due to mass flow rate are included. Although material damping does exist in reality, it is rather difficult to model. Unlike stiffness and mass, which can be quantitatively specified according to material and geometric data, damping has to be determined experimentally. A modal test was conducted by using a hammer impact as input and the two sensor signals as output on a half-inch single straight titanium meter. Q factors were estimated by a circle-fitting method. It was estimated that the Q factor of the drive and Coriolis modes is greater than 3000 (damping ratio less than 0.02%), while the Q factor of the modes which involve the inner cylinder or outer case is less than 200 (damping ratio greater than 0.25%).

With these data, global proportional damping and local material damping was added to the model so that the global damping matrix is

$$\mathbf{C} = \sum_{e} \mathbf{C}^{(e)} + \alpha \mathbf{M} + \beta \mathbf{K} + \sum_{i} \beta_i \mathbf{K}_i \tag{4}$$

where $\mathbf{C}^{(e)}$ is the individual damping matrix for each fluid-tube interaction element; $\mathbf{M}$ and $\mathbf{K}$ are the global mass and stiffness matrices respectively, α and β are constant; and where β_i and $\mathbf{K}_i$ are proportional damping for a local region i (i=1…m). By varying α, β and β_i, a best fit to experimental data can be obtained, and is used in the current model.

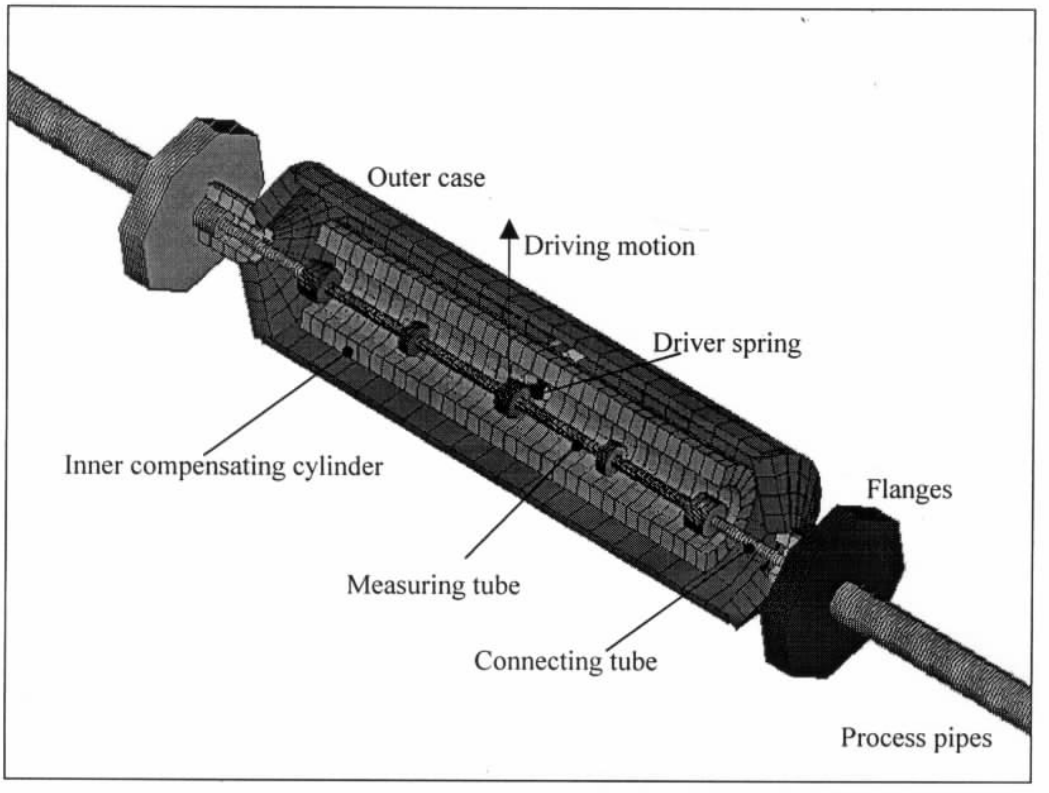

Fig. 2 A section view of the complete finite element model

4. Typical results and discussion

4.1 The validation of the model

Two sizes (one-inch and half-inch) of Krohne Optimass meters were chosen for this study. For each size, meters of two different materials (titanium and stainless steel) were used. Nominal dimensions in the drawings and material properties from the suppliers were used in the current model. The comparison between FEA (finite element analysis) and the statistical data of a number of calibrated meters is shown below.

In Fig. 3, the frequencies of FEA are those resonant frequencies calculated from a free vibration analysis for the drive mode. In order to compare with practical data in normal calibrations, meters were simulated filled with water at room temperature. The error bars represent $\pm 2\sigma$, where σ is the standard deviation of a number of calibrated meters.

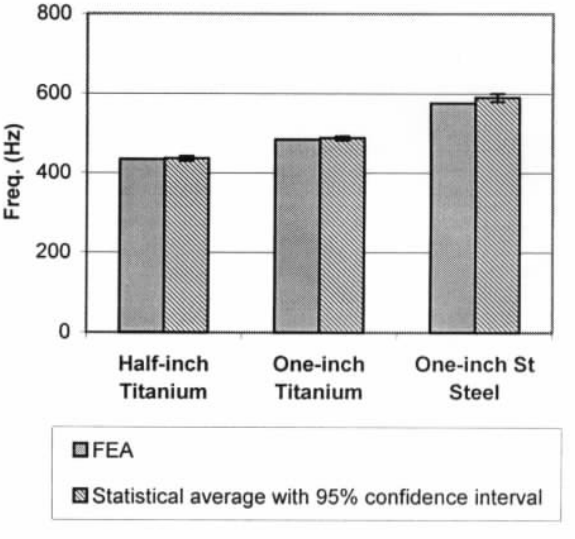

Fig. 3 Comparison of the drive frequency for water

In Fig. 4, the comparison is given in terms of the sensitivity factor, which is defined as phase shift divided by mass flow rate (nanoseconds per kg/s). Again, the simulated fluid was water at its corresponding full scale.

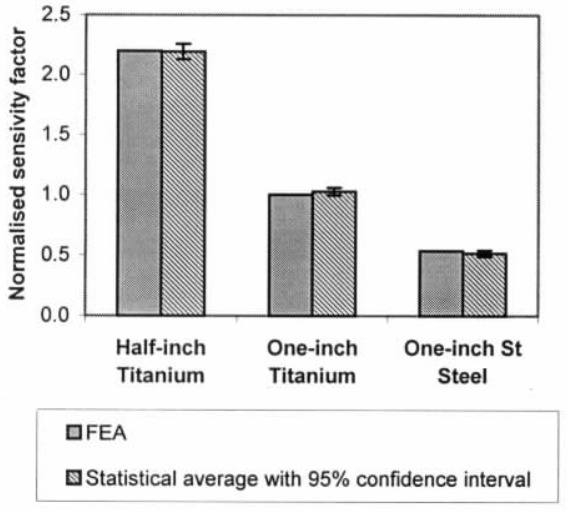

Fig. 4 Comparison of the sensitivity factor for full-scale water flow

4.2 Minimizing the effects of mounting conditions

To minimize the effect of mounting conditions, one of the objectives is to reduce the noise coming from or escaping to the outside environment. A possible solution is the optimization of the stiffness and mass of the connecting tube and inner cylinder. Hussain [10] gave a theoretical explanation and described the Adaptive Sensor Technology (AST).

We modeled a typical titanium meter and used the ratio of the amplitude at the flanges to the amplitude at the driver to characterize the possible noise problem. The comparison between the current design and two modified cases is shown in Fig. 5. In this comparison, the process pipes are clamped at a distance of five times the pipe diameter away from the flanges, and full-scale water flow was simulated. As reported by Hussain [10], the current design appears to provide an optimal combination of stiffness and mass and to achieve good decoupling from the outside world.

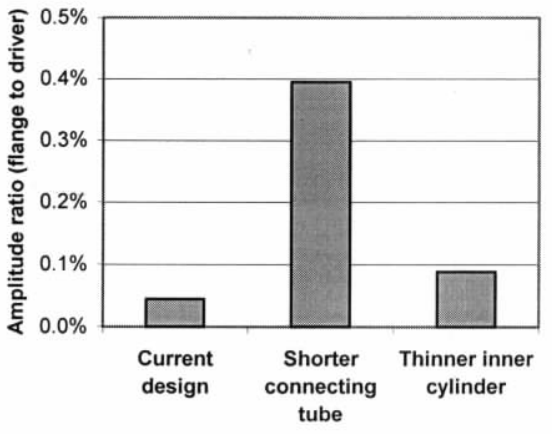

Fig. 5 Comparison of amplitude ratio for three simulated cases

4.3 The effects of a driver spring

The drive frequency and phase shift for variation in the diameter of the driver spring are shown in Fig. 6. It is clear that this is an efficient tool for changing the dynamic behaviour of a meter.

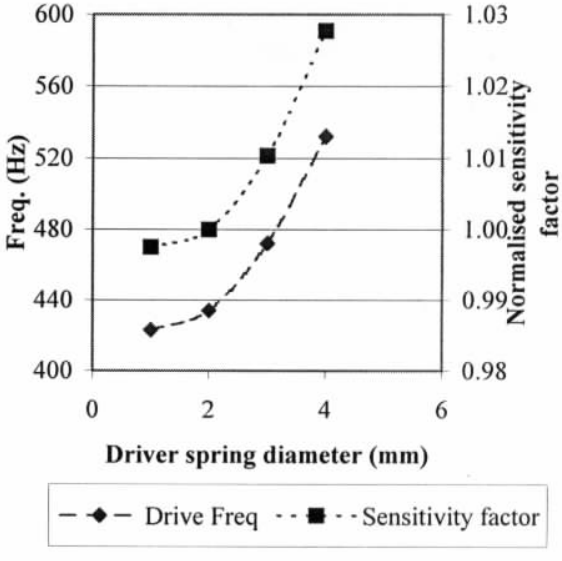

Fig. 6 The effects of a driver spring

6. Conclusions

Our study has shown that the formulated fluid-tube interaction element coupled with conventional structural finite elements can be used as a numerical simulation tool for single straight tube Coriolis flowmeters. The predicted drive frequency and phase

shift agree with the statistical data, which validates the application of this model for further work.

In particular, the function of the compensating cylinder and connecting tube to decouple the measuring tube from the outside world has been demonstrated in a quantitative way by using this model. It has been shown that an optimal combination of stiffness and mass can achieve a metering system relatively insensitive to mounting conditions.

Furthermore, other additional features, such as the driver spring, emphasize the benefit of using a more complete numerical model of the meter design, noting that the simpler theoretical models of single straight tube meters have omitted important features of the real meter.

Acknowledgment

The authors would like to thank Professor Ian Hutchings and Professor Jim Woodhouse of Cambridge University Engineering Department for helpful discussions. Thanks are also due to Jacques van den Bosch, Chris Rolf and Edward Jukes of Krohne Ltd for their assistance with some of the experimental work. The authors also wish to acknowledge support for this work from Krohne Limited, from Knowledge Transfer Partnership funding, and from the Gatsby Charitable Foundation.

References

[1] Raszillier, H. & Durst, F., Coriolis-effect in mass flow metering. Achive of Applied Mechanics, 1991, 61: 92-214.

[2] Kutin, J. & Bajsic, I., Stability-boundary effect in Coriolis meters, Flow measurement and instrumentation, 2001, 12: 65-73

[3] Sultan, G. and Hemp, J., Modelling of the Coriolis mass flowmeter. Journal of Sound and Vibration, 1989. 132(3): p. 473-489

[4] Watt, R.M. Computational modeling of Coriolis mass flowmeters. North Sea Flow Measurement Workshop, East Kilbride, Scotland: NEL, 1990

[5] Stack, C.P., Barnett, R.B., and Pawlas, G.E. A Finite Element for the vibration analysis of a fluid-conveying Timoshenko beam (AIAA-93-1552-CP). in AIAA/ASME Structures, Structural Dynamics and Materials Conference. 1993

[6] Belhadj, A., Cheesewright, R., and Clark, C., The simulation of Coriolis meter response to pulsating flow using a general purpose FE code. Journal of Fluids and Structures, 2000. 14: p. 613-634

[7] Cheesewright, R., Belhadj, A., and Clark, C., Effect of Mechanical vibrations on Coriolis Mass Flow Meters, Journal of Dynamic Systems, Measurement, and Control, 2003. 125: 103-113

[8] Wang, T., Baker, R.C., Manufacturing variation of the measuring tube in a Coriolis flowmeter, IEE Proc.-Sci. Meas. Technol., 2004, 151(3): 201-204

[9] Hussain, Y.A. and Rolph, C.N., Mass flow meter. U.S. Patent 5,365,794, 1994

[10] Hussain, Y.A., Single straight tube mass flowmeters using 'Adaptive Sensor Technology', IEE Seminar on Advanced Coriolis Mass Flow Metering, Oxford, 2003

[11] Hussain, Y.A. and Rolph, C.N., Mass flow meter. U.S. Patent 5,291,792, 1994

[12] Païdoussis, M.P., Fluid-structure Interactions: Slender Structures and Axial Flow, Academic Press, 1998

[13] ANSYS Inc., ANSYS Theory Reference, 2003